Scientia Horticulturae 308 (2023) 111604

Contents lists available at ScienceDirect

Scientia Horticulturae

journal homepage: www.elsevier.com/locate/scihorti

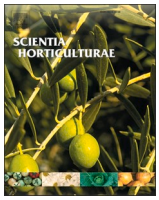

Evaluating late spring frost risks of apple in the Loess Plateau of China under future climate change with phenological modeling approach

Xiaoya Ru [a,b], Yuan Jiang [a,b], Qi Luo [a,b], Runhong Wang [a,b], Xinxin Feng [c], Jinghong Wang [d,e], Zhao Wang [d,e], Meirong Li [d,e], Zhenjiang Qu [d,e], Baofeng Su [f], Hao Feng [g], Dong Zhang [h], Deli Liu [i,j], Qiang Yu [e,g], Jianqiang He [a,b,e,*]

[a] Key Laboratory for Agricultural Soil and Water Engineering in Arid Area of Ministry of Education, Northwest A&F University, Yangling, Shaanxi 712100, China
[b] Institute of Water-Saving Agriculture in Arid Areas of China, Northwest A&F University, Yangling, Shaanxi 712100, China
[c] Nanjing Shuxi Intelligent Technology Co., Ltd., Nanjing, Jiangsu 210019, China
[d] Shaanxi Meteorological Service Center of Agricultural Remote Sensing and Economic Crops, Xi'an, Shaanxi 710014, China
[e] Key Laboratory of Eco-Environment and Meteorology for the Qinling Mountains and Loess Plateau, Shaanxi Provincial Meteorological Bureau, Xi'an, Shaanxi 710015, China
[f] College of Mechanical and Electronic Engineering, Northwest A&F University, Yangling, Shaanxi 712100, China
[g] State Key Laboratory of Soil Erosion and Dryland Farming on the Loess Plateau, Institute of Water and Soil Conservation, Northwest A&F University, Yangling, Shaanxi 712100, China
[h] College of Horticulture, Yangling Subsidiary Center Project of the National Apple Improvement Center, Northwest A&F University, Yangling, Shaanxi 712100, China
[i] New South Wales Department of Primary Industries, Pine Gull Road, Wagga Wagga Agricultural Institute, Wagga Wagga, NSW 2650, Australia
[j] Climate Change Research Centre, University of New South Wales, Sydney, NSW 2052, Australia

ARTICLE INFO

Keywords:
Apple
Fruit-setting
Late-spring frost
Phenology models
Climate change

ABSTRACT

Changes in apple phenology associated with climate change have attracted extensive attention. However, it is poorly known whether the phenological dynamics responding to climate change would increase the severity and frequency of frost in apple trees. Here, we investigated the variation of phenophase (budburst and fruit-setting) and the frost risk for apple trees in the Loess Plateau combined with phenology models driven by Global Climate Models (GCMs) under two emission scenarios (SSP2-RCP4.5 and SSP5-RCP8.5 for two time periods 2050s and 2090s, respectively). The results showed that apple budburst and fruit-setting are expected to be advanced to varying degrees, but the rate of advance is decreasing (budburst 0.04–0.14 d•y^{-1}, fruit-setting 0.12–0.22 d•y^{-1}). The combinations of high emission scenarios and 'far' time periods (SSP5-RCP8.5, 2090s) in budburst and fruit-setting advance larger than conservative emission scenarios and 'near' time periods (SSP2-RCP4.5, 2050s). Furthermore, although frost frequency is expected to decrease about 0.09–0.36 d under both SSP2-RCP4.5 and SSP5-RCP8.5, frost intensity tends to increase about 0.004–0.008 °C·d^{-1} (except SSP5-RCP8.5, 2090s). Due to the different directions of changes in frequency and intensity of frost under future time periods, overall frost risk showed regional differences. The unchanged or decreased frost risk distributed in the northern and southern areas of the study areas, while the increased frost risk mainly distributed across the central areas of the study areas. Finally, the advancement of two phenophase was disproportionately related to frost risks in the geographic distributions. Areas with large advance in phenophase were themselves expected to be at greater frost risk. Our findings will help to promote local preventative interventions for reasonably reducing the risk of late spring frosts in future climate warming scenarios.

1. Introduction

Apple (*Malus domestica* Borkh.) is the fourth most cultivated fruit tree after citrus, grapes, and bananas (Mbovora et al., 2021). The Loess Plateau of China is globally the largest area of intensive apple cultivation, where the planting area and yield of apple trees account for about

* Corresponding author at: Key Laboratory for Agricultural Soil and Water Engineering in Arid Area of Ministry of Education, Northwest A&F University, Yangling, Shaanxi 712100, China.
E-mail address: jianqiang_he@nwsuaf.edu.cn (J. He).

https://doi.org/10.1016/j.scienta.2022.111604
Received 28 February 2022; Received in revised form 5 September 2022; Accepted 8 October 2022
Available online 15 October 2022

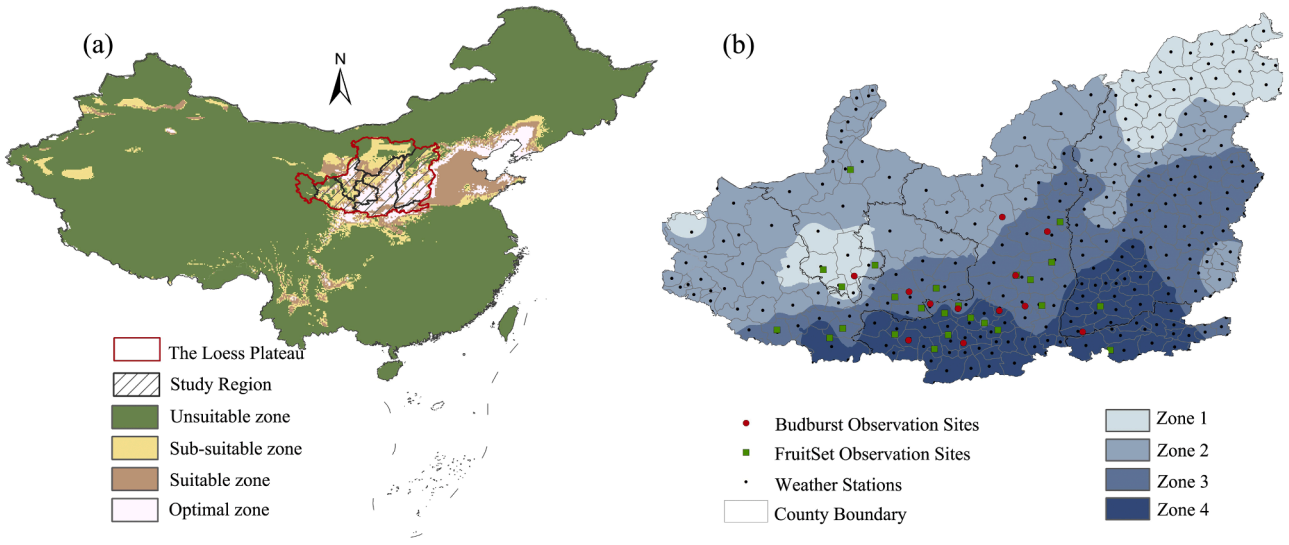

Fig. 1. Climate-suitable growth regions of apple in China (Qu and Zhou, 2016) and the study area (grey shadowed) in the Loess Plateau; (b) spatial distributions of weather stations (black points) and phenology observation sites (red circles and green squares) in the study area. The red circles represented 12 budburst observation sites, and the green squares represented 24 fruit-setting observation sites. Zone 1–4 were the sub-regions divided based on the average temperature.

25.2% and 26.3% of global planting area and production, respectively (Wang et al., 2020b). Among dormancy, budburst, flower, fruit-set and fruit maturity, etc., the development of apples from budburst to fruit-setting plays an important role in final yield and quality formation, but it is very susceptible to frost injury (Farajzadeh et al., 2010; Hoffmann and Rath, 2013). Late-spring frosts, or frost events occurring after budburst of fruit trees could cause more crop losses and more serious economic consequences than any other climate-related disasters (Lamichhane, 2021; Unterberger et al., 2018). For instance, the severe spring frost in early April of 2018 significantly damaged apple production in the Loess Plateau of China, in which about 53.7% of the total apple producing counties became the worst-hit regions. The rate of apple setting fruit decreased by 46% compared with the previous years, which resulted in a 17.9-19.4% reduction of whole apple production (Qiu et al., 2020; Wang et al., 2020a). Recently, some studies have evaluated late-spring frost for apples and supposed that frost risk cannot be reduced by the end of the 21st century (Farajzadeh et al., 2010; Guo et al., 2019; Hoffmann and Rath, 2013). Frost often occurs in the Loess Plateau under the current climate. Whether it will suffer frost risk that cannot be reduced and even increased in future climate change is of great significance to the local apple production. Therefore, it is urgent to assess the change of late spring frost in apples on the Loess Plateau.

Shifts of spring apple phenophases reflected evident biotic responses of apple trees to global warming. Usually, the internal circadian clock of apple trees that triggers spring phenology mainly depends on the temperature during winter and spring (Pfleiderer et al., 2019). Cold winter temperatures (chilling temperatures) were known to break endo- and ecodormancy (Zhang et al., 2021), while warm spring temperatures (forcing temperatures) were known to promote growth in flower buds (Dennis, 2003). Usually, temperature below 7.2 °C was regarded as effective chilling temperatures for apples, and most apple varieties required 500-1000 h of the effective chilling to break endo- and ecodormancy (Weinberger, 1950; Powell, 1986; Hawerroth et al., 2013). Moreover, temperature from 12.8 to 40 °C was also proved as effective forcing temperatures for apple trees (Heide and Prestrud, 2005; Yaacoubi et al., 2019). When the effective forcing exposure reached the required time, particular physiological stage such as budburst, flowering, and fruit-setting of apple trees was initiated (Yaacoubi et al., 2019). Recently, with increasing warm temperatures in late winter or early spring, phenology was accelerated. This resulted in a false spring wherein apples break endo- and ecodormancy and begin their annual development earlier than normal, thereby raising the risk of damage from subsequent frost exposure (Liu and Sherif, 2019; Parker et al., 2020). However, the variations in cultivars, phenological periods, and threshold of frost (e.g., 0 °C) a global assessment of spring frost damage to apple trees were still in an exploratory stage (Darbyshire et al., 2016a; Houston et al., 2017; Masaki, 2019). Combined with changes in apple phenology, several studies reported that frost risk was projected to remain unchanged or increase in south-eastern Styria (Unterberger et al., 2018), to increase in United Kingdom (Smith, 1986), Finland (Kaukoranta et al., 2010) and the United States (Labe et al., 2016), while to decrease in Germany (Hoffmann and Rath, 2013) and Shaanxi province of China (Guo et al. 2019). These differences suggested that there was still debated globally, although the phenological dynamics in apple trees have an impact on the potential frosts.

The most fundamental method to assess frost injury was to conduct experiments in different growing areas with various tree species, but this was a very difficult task, subject to restrictions such as reproducing the daily variability of climate warming scenarios in situ, following frost damage on live tissues, etc (Xavier and Isabelle, 2014). Another more efficient method was to establish models to predict phenology and frost risk (Eccel et al., 2009; Guillaume et al., 2018; Smith, 1986), by coupling climate models and scenarios to reveal long-term climate change impacts. This modeling approach was reported widely due to it providing a possibility for regional-scale evaluation of spring frost risks. For instance, Hoffmann and Rath (2013) and Pfleiderer et al. (2019) applied phenological models coupling climate models to project the blooming stage and frost risk for apples in Germany. They agreed that the phenophase of apples would earlier in the future, but hold different opinions about frost risk. The former argued frost cannot be expected to increase under warmer climate, while the latter argued frost risk would increase. The reason for this discrepancy was most likely due to the different types of models, including phenological model and climate model. Different model structures, parameterizations, and assumptions would result in different outcomes (Yan et al., 2021), although analyzing similar phenophase in the same region. Furthermore, all kinds of models present uncertainties. For instance, uncertainties and errors in modeled variables themselves, and uncertainties in different calibration algorithms (Yan et al., 2021). Given these uncertainties on phenology modeling (Darbyshire et al., 2016b; Migliavacca et al., 2012), we considered integrating several models to provide final phenological estimates. In addition to more robust phenological predictions, trustworthy local

Table 1
Functions about four models and description of parameters used to perform phenology estimates in this study. DOY = Day of the year (31DOY refers to Jan. 1; -67DOY refers to Oct. 26); R_f = daily sum of rates of forcing; R_c = daily sum of rates of chilling; T_i = the response temperature to forcing of the Julian day i; T_j = the response temperature to forcing of the Julian day j.

Models	Functions	Parameters	Description(Units)	Refs.
Uniforc	$\sum_{t=t_1}^{DOY} R_f(T_i) \geq F^*$ (1) $R_f(T_i) = \frac{1}{1+e^{b(T_i-c)}}$ (2)	t_1 F* b c	The DOY which forcing accumulating beings The total forcing units required Sigmoid function parameter Sigmoid function parameter	(Chuine 2000)
Unichill	$\sum_{t_1}^{DOY} R_f(T_i) \geq F^*$ (3) $\sum_{t_0}^{t_c} R_c(T_j) \geq C^*$ (4) $R_f(T_i) = \frac{1}{1+e^{b\_f(T_i-c\_f)}}$ (5) $R_c(T_j) = \frac{1}{1+e^{a\_c(T_i-c\_c)^2+b\_c(T_i-c\_c)}}$ (6)	t_0 C* F* b_f c_f a_c b_c c_c	The DOY which chilling accumulating beings The total chilling units required The total forcing units required Sigmoid function parameter for forcing Sigmoid function parameter for forcing Sigmoid function parameter for chilling Sigmoid function parameter for chilling Sigmoid function parameter for chilling	(Chuine, 2000; Kramer, 1994)
Alternating	$\sum_{t_1}^{DOY} R_f(T_i) \geq a + be^{c(t)}$ (7) $R_f(T_i) = \max(T_i - threshold, 0)$ (8)	t_1 threshold a b c	The DOY which forcing accumulation starts. Degree threshold above which forcing accumulates, and below which chilling accumulates. Intercept of chill day curve Slope of chill day curve scale parameter of chill day curve	(Cannell and Smith, 1983)
M1	$\sum_{t_1}^{DOY} R_f(T_i) \geq (L_i/24)^k F^*$ (9) $R_f(T_i) = \max(T_i - threshold, 0)$ (10)	t_1 T F* k	The DOY which forcing accumulating beings The threshold above which forcing accumulates The total forcing units required Daylength coefficient	(Blümel and Chmielewski, 2012)

climate predictions are also required. Therefore multiple climate models were also used to reduce model-induced uncertainties.

In this study, taking into account the whole phenophase of apple trees in spring, we focused on evaluating the phenological dynamics and late-spring frost risk on apple trees (Malus domestica Borkh. cv. Fuji) in the Loess Plateau of China. Four phenological models were driven by 27 Global Climate Models (GCMs) to assess changes in phenology. Then, two frost indices AFD (accumulated frost days) and AFDD (accumulated frost degree-days), as proxies for frost frequency and intensity, were used to quantify late-spring frosts under climate change. The detailed objectives were to (1) assess the accuracy and reliability of the four phenological models used for apple budburst and fruit-setting date predictions; (2) analyze the spatial and temporal changes of apple budburst and fruit-setting dates under future climate; (3) quantify the frequency and intensity of late-spring frost occurrence from budburst to fruit-setting stage based on AFD and AFDD under future climate.

2. Materials and methods

2.1. Study area

There are four major apple producing areas in China: the Loess Plateau (33°−41°N, 100°−114°E), the Bohai Bay Area (35°−43°N, 113°−124°E), the Southwest Cold Highlands (23°−29°N, 99°−106°E), and Xinjiang province (35°−50°N, 75°−95°E). This study focused on the Loess Plateau, where is the largest dominant apple-growing area in China (Fig. 1a). This region has high climate suitability for apple cultivation (Qu and Zhou, 2016), and *'Fuji'* apple is the main local variety. After removing parts of the regions without planting apples (areas not filled with shadows in the Loess Plateau in Fig. 1a), the whole region includes 113 main apple-producing counties, and the location is listed in Table S1. Based on temperatures, the whole study area was divided into four sub-regions (Zones 1−4 in Fig. 1b).

2.2. Data collection

The *'Fuji'* apple phenology dataset mainly included dates of budburst and fruit-setting at different observation sites. The budburst date was defined as one-half inch of the bright green tissue is projecting from buds (Chapman and Catlin, 1976). The fruit-setting date was defined as the date on which 5% of apple young fruits clearly grew on the branches after the petals fell off (Chapman and Catlin, 1976). These phenology observation data were mainly obtained from the Shaanxi Meteorological Bureau (2017) (http://sn.cma.gov.cn/) and the Shaanxi Fruits Industry (2014) (http://www.guoye.sn.cn/). In total, we obtained budburst date data for 12 different sites in 1972−2018 and fruit-setting date data for 24 different sites in 2016−2020 (Fig. 1b and Table S2). These data were

Table 2
Information about the 27 GCMs used in this study under the future climate scenarios of SSP2-RCP4.5 and the SSP5-RCP8.5. The original grid-scale data were converted to site-scale data for the 113 sites in the Loess Plateau based on statistical downscaling methods (Liu and Zuo, 2012).

No.	Name of the GCM	Abbreviation	Institute	Country
1	ACCESS-CM2	ACC1	CSIRO-ACCESS	Australia
2	ACCESS-ESM1-5	ACC2	CSIRO-ACCESS	Australia
3	BCC-CSM2-MR	BCCC	BCC	China
4	CanESM5	Can1	CCCma	Canada
5	CanESM5-CanOE	Can2	CCCma	Canada
6	CIESM	CIES	THU	China
7	CMCC-CM2-SR5	CMCS	CMCC	Italy
8	CNRM-CM6-1	CNR2	CNRM-CERFACS	France
9	CNRM-CM6-1-HR	CNR3	CNRM-CERFACS	France
10	CNRM-ESM2-1	CNR1	CNRM-CERFACS	France
11	EC-Earth3	ECE1	EC-EARTH-Consortium	Europe
12	EC-Earth3-Veg	ECE2	EC-EARTH-Consortium	Europe
13	FGOALS-g3	FGOA	CAS	China
14	GFDL-CM4	GFD1	NOAA-GFDL	USA
15	GFDL-ESM4	GFD2	NOAA-GFDL	USA
16	GISS-E2-1-G	GISS	NASA-GISS	USA
17	HadGEM3-GC31-LL	HadG	MOHC	UK
18	INM-CM4-8	INM1	INM	Rusia
19	INM-CM5-0	INM2	INM	Rusia
20	IPSL-CM6A-LR	IPSL	IPSL	France
21	MIROC6	MIR1	MIROC	Japan
22	MIROC-ES2L	MIR2	MIROC	Japan
23	MPI-ESM1-2-HR	MPI1	MPI-M	Germany
24	MPI-ESM1-2-LR	MPI2	MPI-M	Germany
25	MRI-ESM2-0	MTIE	MRI	Japan
26	NESM3	NESM	NUIST	China
27	UKESM1-0-LL	UKES	MOHC	UK

mainly used to calibrate and verify the phenological models to predict budburst and fruit-setting of apple trees. Based on temperature, the whole study area was divided into four sub-regions (Zones 1−4 in Fig. 1b) for more accurate simulations of apple phenological events. Additionally, daily weather data (air temperature and sunshine hour) were obtained from The National Meteorological Information Center (2014) (http://data.cma.cn/) for the 113 main apple-producing counties located in the Loess Plateau in 1981-2020 (Baseline).

2.3. Phenological models

Our study used the '*pyPheonology*' package (0.7.1 version) in the Python language to run the relevant phenology models (Taylor, 2018). The package has an object-oriented API where the same analysis code can be used regardless of the underlying model. '*pyPheonology*' package included nine process-based spring phenology models, one simple linear regression model and one fall senescence model. These models are differed by implemented processes and drivers: chilling temperatures, forcing temperatures, and photoperiod (Hufkens et al., 2018). We selected four spring phenology models (Uniforc, Unichill, Alternating, and M1 model). A list of the model mathematical functions, parameters, and descriptions for models are provided in Table 1. Uniforc and M1 models are common forcing-driven models, while Unichill and Alternating models are driven by both forcing and chilling temperatures. In particular, the effective threshold temperature of chilling in Unichill and Alternating models is crucial for triggering budburst and fruit-setting events in apple growing. Several threshold temperatures have been suggested as the upper limit for chilling efficacy in apples. For instance, -2−16.8℃ in Okanagan (Guak and Neilsen, 2013) and -2−12℃ in Germany (Kaufmann and Blanke, 2019). Generally, the most effective temperatures in dormancy completion for apples are between -2 and 5.5 ℃ (Guak and Neilsen, 2013). However, this effective chilling temperature was known to vary depending on cultivar or locality (Baumgarten et al., 2021; Zhang et al., 2021). To determine the thresholds, we checked different temperature range from -5 to 15°C with interval of 5 °C to test the model performance. Due to the effective threshold values are not fixed in Unichill model as usually assumed, which response function is always effective below a certain threshold temperature or a range of temperatures (Fig. S1). Thus, we employed the Alternating model to make this test. The temperature below 5 °C was finally chosen as the effective threshold. The test results and analysis were provided in Supplemental Information section (Fig. S2).

2.3.1. Uniforc model

The model is a one-phase model (Equations 1-2), describing the cumulative effect of forcing temperatures on the development of buds during the ecodormancy phase (Chuine, 2000). It assumes that the endodormancy phase is always fully released and that chilling and photoperiod have no dynamic effects on forcing requirements (Chuine, 2000).

2.3.2. Unichill model

The model is a sequential two-phase model (Equations 3-6) describing the cumulative effect of chilling temperatures on the development of buds during the endodormancy phase and the cumulative effect of forcing temperatures during the ecodormancy phase, which assumes that the phase of bud growth starts only when endodormancy break has occurred (Chuine, 2000).

2.3.3. Alternating model

The Alternating model is also a two-phase model, but the two phases can overlap in process (Equations 7-8). It assumes that the ecodormancy phase can start before the end of endodormancy phase, or before endodormancy break (Cannell and Smith, 1983). Phenological event happens the first day that forcing is greater than an exponential curve of number of chill days (Cannell and Smith, 1983).

2.3.4. M1 model

The M1 model is the Thermal Time Model (Cannell and Smith, 1983) with a daylength correction (Equations 9-10). It means the model requires a daylength column in the predictors in addition to daily temperature (Blümel and Chmielewski, 2012). The daylength depends on the day of the year and the geographical latitude.

2.4. Model parameter optimization and validation

To parameterize phenological models, we fitted each model for each zone (Zones 1-4 in Fig 1b) to the pooled dataset of all years and sites. Fitting was performed through basin hopping algorithm (Wales and Doye, 1997), minimizing the root mean square error (RMSE) between the 70% observed and simulated dates of the pooled dataset in each zone. Basin hopping algorithm first made a random guess for parameter values, then searched the local minima through the L-BFGS-B algorithm (Byrd et al., 1995). Then from the local minima, the parameters were randomly perturbed and minimized again. The new estimates were accepted based on the Metropolis criterion (Gubernatis, 2005; Hastings, 1970). The parameters with the minimum RMSE were finally selected. Basin hopping was described in more detail by David Wales and Jonathan Doye (Wales and Doye, 1997). Given the model effect and time cost, we set the number of iterations to 1000 and the random perturbations to 0.5 for basin hopping algorithm. In addition, to assess the robustness of the models, the remaining 30% observation from the original sample was used as the validation datum using the above-calibrated best parameter sets. We compared the models' accuracies on the basis of the adjusted R square (R^2) and root mean square error (RMSE) calculated for both the fit on the whole pooled data set following equations (Eqs. (11) and (12):

$$R^2 = 1 - \frac{\sum_i (O_i - P_i)^2}{\sum_i (O_i - \overline{O}_i)^2} \tag{11}$$

$$RMSE = \sqrt{\frac{\sum_{i=1}^{n} (O_i - P_i)^2}{n}} \tag{12}$$

where O_i represented observed apple phenology dates (DOY); $\overline{O}$ represented the average observed phenology dates (DOY); P_i represented simulated phenology dates at site *i*; *n* was the number of observations.

2.5. Future climate dataset

Future monthly gridded climate data were downloaded for 27 GCMs (Table 1) utilized in Coupled Model Intercomparison Project Phase (2021) (https://esgf-node.llnl.gov/projects/cmip6/) - Intergovernmental Panel on Climate Change - Sixth Assessment Report (CMIP6 IPCC AR6) as discussed by Eyring et al. (2016). Recently, IPCC AR6 advocated five different new scenarios coupling the Shared Socioeconomic Pathways (SSPs) and Representative Concentration Pathways (RCPs), namely SSP1-RCP1.9, SSP1-RCP2.6, SSP2-RCP4.5, SSP3-RCP7.0, SSP5-RCP8.5 (IPCC 2021). To provide both a conservative and comparatively larger estimate of potential climate change, we focused on data from future scenarios run under SSP2-RCP4.5 (conservative) and SSP5-RCP8.5 (high). Our analysis considered the contemporary climatological period (1981–2020) and two future time periods 2050s (2021–2060) and 2090s (2061–2100).

The future monthly climate data (spatial resolution 1°) were spatiotemporally downscaled to daily scale by a weather generator based statistical downscaling approach developed by NSW Department of Primary Industries at Wagga Wagga Agricultural Institute (NWAI-WG) (Liu and Zuo, 2012). This downscaling process consisted of spatial downscaling and temporal downscaling. The first step was to interpolate

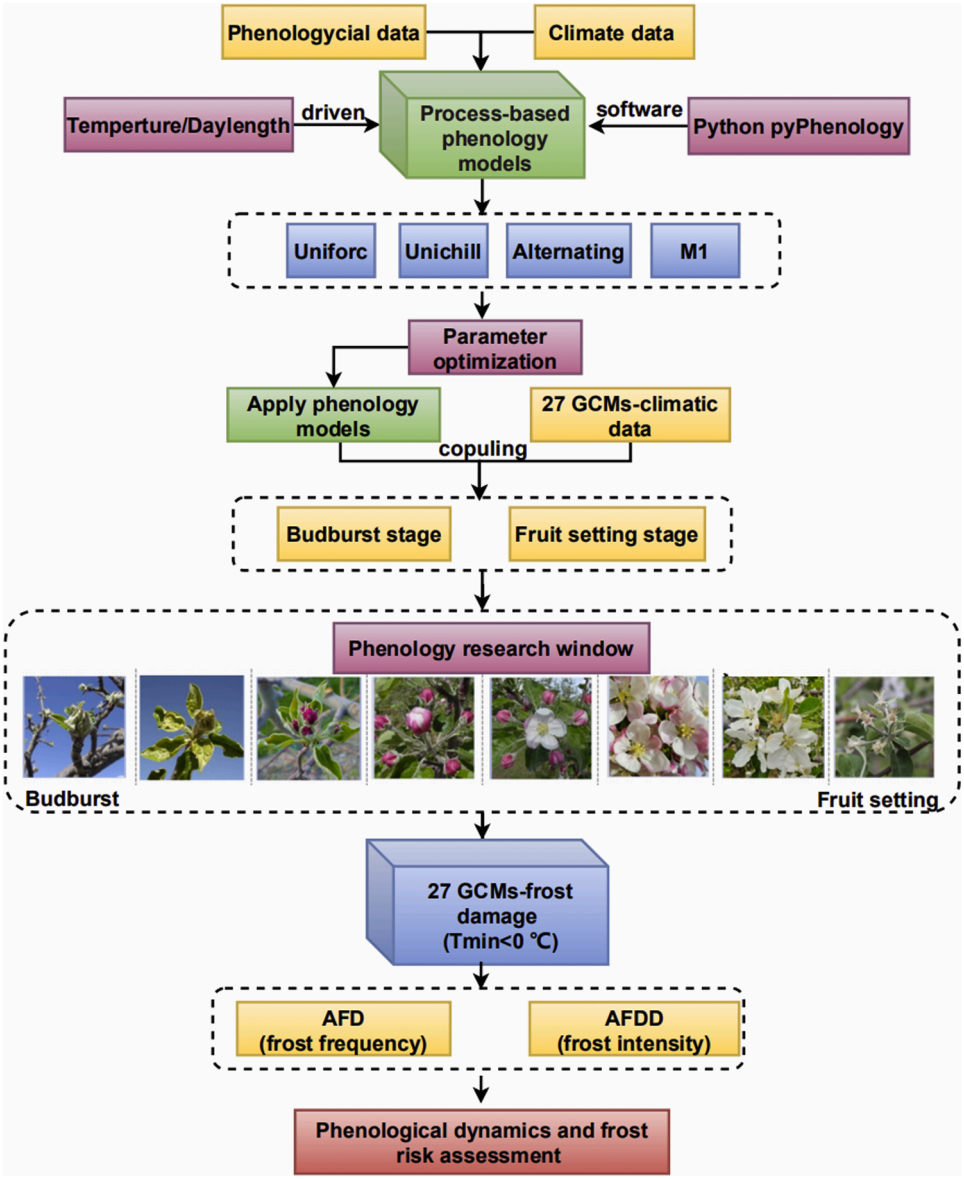

Fig. 2. Framework of this study.

the monthly projections of climate variables from GCMs grid cells to monthly values for each of the sites of interest using an inverse distance-weighted method (Liu and Zuo, 2012). Then, bias correction was applied to enable the resulting monthly site data to match with the observed data using a quantile mapping technique (Zhang, 2007). The second step was to disaggregate the monthly data to daily data through the modified WGEN stochastic weather generator (Liu and Zuo, 2012).

2.6. Apple phenology projections and late-spring frosts evaluation

The framework for projections of apple phenophase (budburst and fruit-setting) and the quantification of late-spring frost risk are shown in Fig 2. After model optimization (Section 2.4), a set of parameters with the smallest error (RMSE) of Zones 1-4 for each model was selected to estimate how climate change may alter budburst and fruit-setting under SSP2-RCP4.5 and SSP5-RCP8.5 scenarios. Each phenological model driven by each GCM was used to simulate the two phenophase, then we calculated the average simulation results of the four models as the final phenological prediction. According to the prediction of budburst to fruit-setting, we calculated the phenological sensitivity window of apple trees, and quantified frost risk during the window period. These results including phenology projections and frost risk were finally interpolated to show the spatial variations through the inverse distance weighted method in ArcGIS 10.6. Moreover, annual trends were calculated by fitting the time series of a given phenophase across all stations in the study area in future time periods.

The criteria of minimum air temperature below 0 °C ($T_{min} < 0$ °C) were used to estimate spring frost risk. The threshold of 0 °C was widely reported in previous studies, which was regarded as a simple and effective measure of radiation frost that occurred when the surface temperature of plant organs and tissues was lower than air temperature at standard meteorological conditions (Cannell, 1986; Eccel et al., 2009). Two indices of accumulated frost days (AFD) and accumulated frost degree-days (AFDD) were defined as proxies for frost risk dynamics. The index of AFD (Eq. (13)) was the quantification of frost duration or frost frequency, which was defined as the accumulated days when T_{min} was below 0 °C from apple budburst to fruit-setting stage (Mosedale et al., 2015; Zheng et al., 2015). The index of AFDD (Eq. (14)) was defined as the mean of the accumulated temperature lower than the frost threshold from apple budburst to fruit-setting dates, which was a

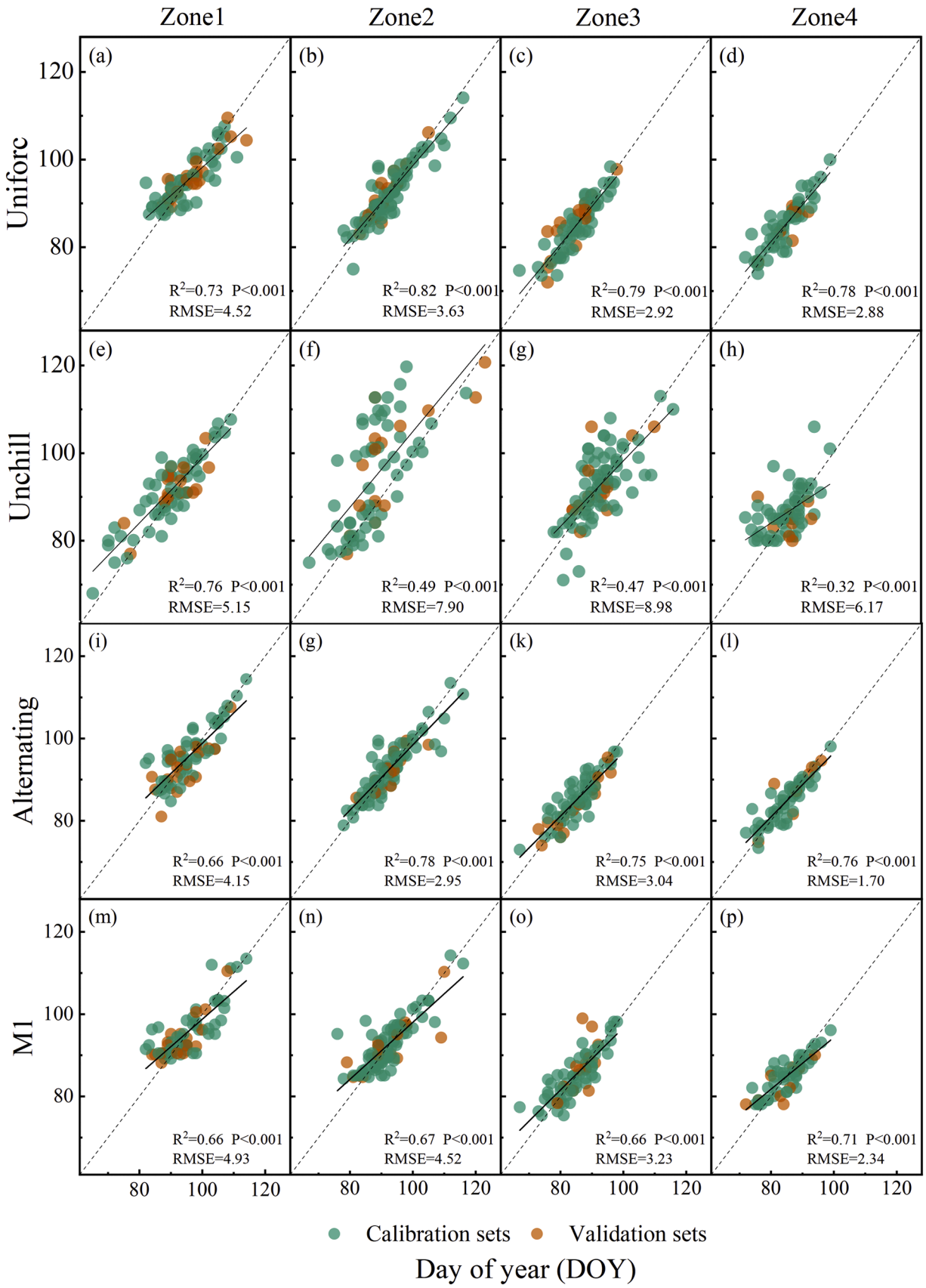

Fig. 3. Observed and predicted apple budburst dates (DOY) with the Uniforc, UniChill, Alternating, and M1 models in the processes of model calibration (red filled circles) and validation (orange filled circles) in the Zone 1 (a, e, i, m), Zone 2 (b, f, g, n), Zone 3 (c, g, k, o), and Zone 4 (d, h, l, p) in the apple production region in the Loess Plateau. The black dotted lines were the 1:1 line. The black solid line was the fitted line.

Table 3
Different parameter sets of the four phenology models used for the prediction of apple budburst dates in the four sub-zones in the apple production region in the Loess Plateau.

Model name	Parameters	Zone 1	Zone 2	Zone 3	Zone 4
Uniforc	t1	46.1	57.82	50.67	50.09
	F*	3851	2599	2077	2018
	b	-1.82	-11.41	-0.58	-0.52
	c	-0.36	2.32	4.81	4.97
Unichill	t0	-73	-73	-73	-73
	C*	600	600	600	600
	F*	10.9	6.18	19.46	15.16
	b_f	-5.08	-8.91	-0.21	-5.98
	c_f	3.77	7.83	5.01	5.7
	a_c	1.16	1.88	0.16	1.66
	b_c	-18.18	12.45	-13.82	14.91
	c_c	-1.23	11.22	-39.81	12.31
Alternating	t1	1	1	1	1
	threshold	5	5	5	5
	a	93.51	142.23	196.48	132.4
	b	3696.03	3143.55	1506.42	1422.28
	c	-0.05	-0.06	-1.59	-0.05
M1	t1	40.07	61.81	55.02	55.17
	T	1.32	2.26	0.522	-21.51
	F*	207.08	182.31	177.34	191.79
	k	41.91	42.46	5.74	11.2

robust index in frost intensity estimation (Deng et al., 2020). It represented the severity and duration of frost stress. Also, AFDD indicated that freezing injury intensity was both affected by temperature and phenological changes of apple trees (Xiao et al., 2018).

$$AFD = \sum_{budburst}^{fruitset} Frostdays_{(T_{\min}<0)} \tag{13}$$

$$AFDD = \frac{\sum_{budburst}^{fruitset} Max(0 - T_{\min},\ 0)}{fruitset - budburst} \tag{14}$$

3. Results

3.1. Model calibration performances

Budburst dates had R^2 of 0.32−0.82 and RMSE of 1.70−8.98 d (Fig. 3). Specifically, the Uniforc and Alternating models were able to explain about 73−82% and 66−78% of the variations of budburst dates in the four zones, respectively. The two models could also provide smaller RMSE (2.88−4.52 d). The Unichill and M1 models could explain about 32−76% and 66−71% of the variations of budburst dates. The corresponding RMSE values were 5.15−8.98 d and 2.34−4.93 d, respectively. Fruit-setting dates had R^2 of 0.33−0.84 and RMSE of 2.97−7.76 d (Fig. S3). The Alternating model had the smallest RMSE (3.69−6.90 d) and could explain about 75−84% of the variations in fruit-setting dates in Zones 2-4, but only about 38% in Zone 1. The Unichill model had RMSE of 2.97−7.10 d and could explain about 52−63% variations in Zones 2-4, but only about 33% in Zone 1. The Uniforc model had RMSE of 5.50−7.75 d and could explain about 65% variations in Zone 4, but only about 35−44% in Zones 1-3. The M1 model had RMSE of 4.98−7.70 d and could explain about 56−77% variations in all zones. As expected, all models provided acceptable estimates for apple budburst dates. Parameter estimates obtained for each model are provided in Table 3.

3.2. Changes of apple budburst and fruit-setting dates under future climates

The budburst dates, which were projected by phenology models in future periods, were compared with those in the baseline in the Loess Plateau (Fig. 4). In the baseline, multi-model averaged budburst dates decreased northward and southward from central part of the study area, with average values about 75−99 DOY and 80−100 DOY under the scenarios of SSP2-RCP4.5 and SSP5-RCP8.5, respectively (Fig. 4a and b). Compared with the baseline, budburst dates were projected to advance in 2050s both under SSP2-RCP4.5 and SSP5-RCP8.5, with mean advancing days about 4.00 d and 4.39 d, respectively (Fig. 4c and d). In 2090s, budburst dates were projected to mean advance about 4.29 d and 8.24 d under SSP2-RCP4.5 and SSP5-RCP8.5, respectively (Fig. 4e and f). However, projected budburst dates would not always advance. For example, budburst dates were projected to mean delay about 3.6 d in 2090s under SSP5-RCP8.5. It was noteworthy that the areas with larger change of budburst date in future period almost overlapped the areas with late budburst dates in the baseline period. For example, budburst dates in baseline period were about 93−100 DOY in counties such as Jingchuan, Xifeng, Zhenyuan, Changwu, Ning, Lingtai, Xunyi, Zhengning, Huangling, and Luochuan. These counties advanced more than 6 d in 2050s under SSP2-RCP4.5, and more than 8 d in 2090s under SSP5-RCP8.5. Spatial variations of apple fruit-setting dates were similar to those of apple budburst dates (Fig. S4).

The advancement rates of apple budburst and fruit-setting dates were further analyzed under the two scenarios (Fig. 5). The average change rate of the budburst date was negative values under two scenarios, indicating an advancing trend. The rank of average advancement rate of budburst under SSP2-RCP4.5 was: baseline (0.14 d•y^{-1}) > 2050s (0.05 d•y^{-1}) > 2090s (0.04 d•y^{-1}). These showed that the advancement of apple budburst would become slower in the future. Under SSP5-RCP8.5, the average change rates were -0.08, -0.04, and 0.06 d•y^{-1} for baseline, 2050s, and 2090s, respectively. A delaying trend was also detected in budburst (Fig. 5a, b). The average change rates of fruit-setting date were about -0.22, -0.15, and -0.12 d•y^{-1} for baseline, 2050s, and 2090s under SSP2-RCP4.5, respectively. The average change rates of fruit-setting date were about -0.22, -0.21, and 0.0026 d•y^{-1} for baseline, 2050s, and 2090s under SSP5-RCP8.5, respectively (Fig. 5c, d). Similar to the budburst, the advance rates of fruit-setting in 2090s were smaller than in 2050s. However, the advance rates of fruit-setting dates were slower than the budburst.

3.3. Spatial-temporal changes of late-spring frost

Spatial variation of AFD from budburst to fruit-setting is shown in Fig. 6. In the baseline, the most frequent frost with the highest value was observed in middle region of Shaanxi province, with the maximum value of 7.6 d for AFD. In contrast, the minimum AFD was 0.018 d in southern parts of Shaanxi. The AFD values in about 58.41% of the sites were less than 0.43 d, indicating that the frequency of frost was at a low level in more than half of the Loess Plateau during the baseline period (Fig. 6a, b). In 2050s, about 62.83% and 76.11% of the sites showed a decreasing trend for AFD under SSP2-RCP4.5 and SSP5-RCP8.5 (Fig. 6c, d). In 2090s, the sites that still decreased were up to 85.84% and 87.61% under two scenarios, respectively (Fig. 6e, f). For scenarios, the average AFD decreased up to 0.13 d and 0.09 d in 2050s and 2090s under SSP2-RCP4.5 (Fig. 6c, e). And the average AFD decreased up to 0.27 d and 0.36 d in 2050s and 2090s under SSP5-RCP8.5 (Fig. 6d, f). This showed that frost is expected to occur less frequently under the SSP5-RCP8.5 than SSP2-RCP4.5 on average. The largest decrease occurred in the southern part of the study area with a maximum decrease of 1.75 d higher than the northwest region (0.4−1.2 d) under SSP5-RCP8.5.

Similar spatial distribution of AFDD with AFD was found in baseline period (Fig. 7). Although the average AFDD was 0.05 °C·d^{-1}, the severe frost intensity was observed in some central areas with the maximum AFDD up to 0.34 °C·d^{-1} (Fig. 7a, b). Compared with the baseline, the average AFDD increased by 0.008 °C·d^{-1} and 0.004 °C·d^{-1} in 2050s under the two scenarios (Fig. 7c, d), indicating that the intensity of frost increased in the Loess Plateau. By 2090s, the average AFDD continued to increase by 0.008 °C·d^{-1} under SSP2-RCP4.5, but decreased 0.002

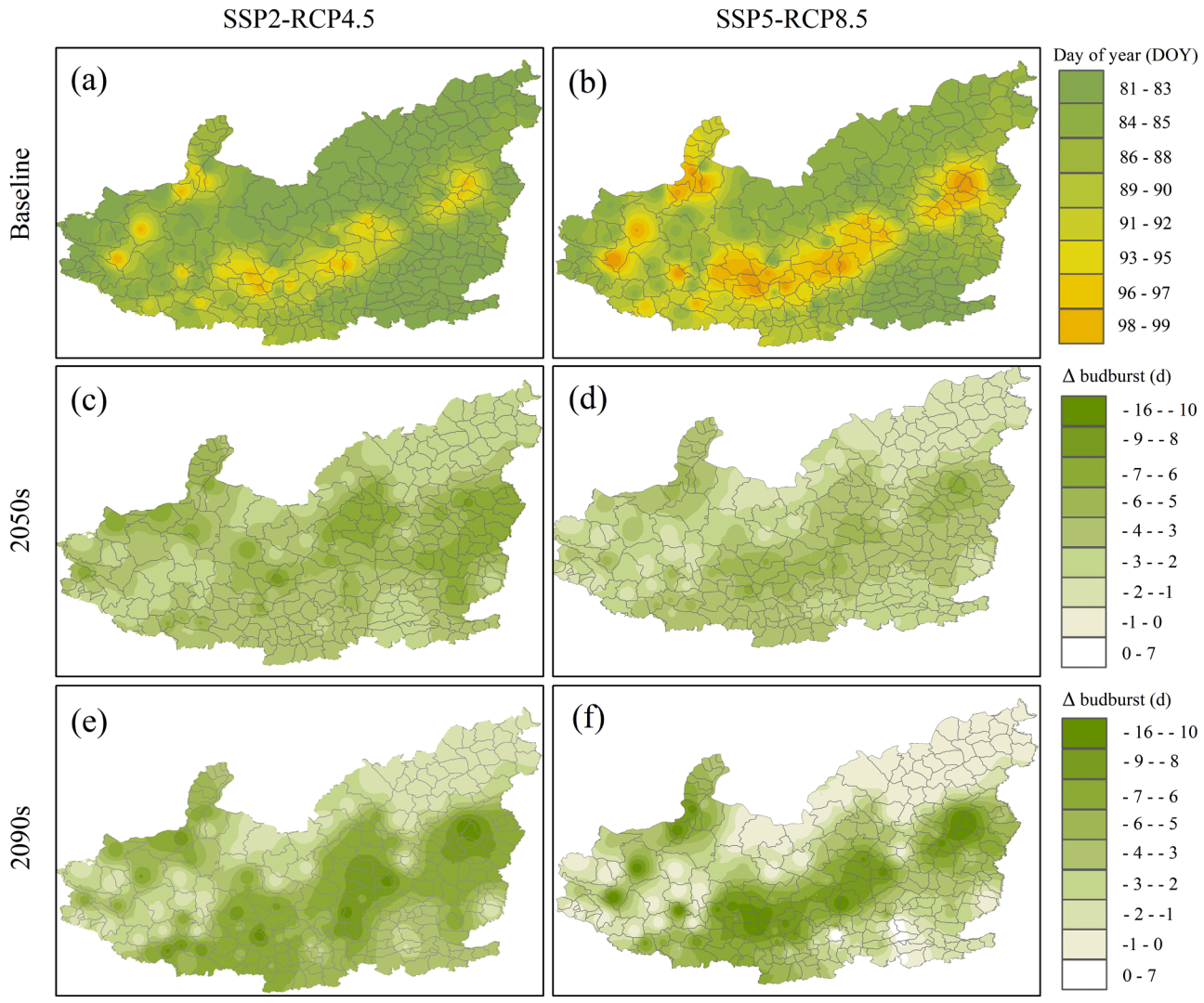

Fig. 4. Spatial distributions of apple budburst dates in the baseline of 1981-2020 (a-b) and average changes of budburst dates in 2050s (2021-2060, c-d) and 2090s (2061-2100, e-f) projected by an ensemble of multiple phenology models driven by 27 GCMs under the SSP2-RCP4.5 and SSP5-RCP8.5 scenarios in apple production region in the Loess Plateau. Changes of apple budburst dates were defined as the differences of projected dates between the baseline and the future (Δ budburst= future-baseline).

$^{\circ}C{\cdot}d^{-1}$ under SSP5-RCP8.5 (Fig. 7e, f). Regional analysis suggested about 74.34% and 69.03% of the sites showed an increasing trend for AFDD in 2050s higher than 50.44% and 24.78% in 2090s under SSP2-RCP4.5 and SSP5-RCP8.5. This showed an increase in AFDD in over 70% of the sites in 2050s compared to the baseline period, and the percentage of these sites decreased in 2090s, especially decreased by nearly 44% under SSP5-RCP8.5. In the entire region, the reduction in AFD did not mean AFDD would decrease. For instance the AFD and AFDD was -0.75 d and 0.008 $^{\circ}C{\cdot}d^{-1}$ in Yuzhong in 2090s under SSP2-RCP4.5, respectively (Fig. 6 and Fig. 7).

4. Discussion

4.1. Performances of phenology models

All model errors of budburst and fruit-setting dates were below 8.98 and 7.76 d, respectively, which were in the range of published model performances (Eccel et al., 2009; Hoffmann and Rath, 2013; Kaukoranta et al., 2010; Masaki, 2019). However, there was no single best individual model that outperformed in all zones. For instance, the Uniforc model outperformed other models in Zone 4 (R^2 0.78, RMSE 2.88 d) for budburst estimation and in Zone 3 (R^2 0.44, RMSE 5.50 d) for fruit-setting estimation. The Unchill model outperformed other models in Zone 1 (R^2 0.76, RMSE 5.15 d) for budburst estimation and Zone 3 (R^2 0.53, RMSE 3.29 d) for fruit-setting estimation. The Alternating model outperformed other models in Zone 4 (R^2 0.76, RMSE 1.70 d) for budburst estimation and in Zone 3 (R^2 0.74, RMSE 3.29 d) for fruit-setting estimation. The M1 model outperformed in Zone 4 (R^2 0.71, RMSE 2.34 d) for budburst estimation and Zone 1 (R^2 0.65, RMSE 4.98 d) for fruit-setting estimation. These differences in model performance are likely to hide the variability associated with the use of different GCM under climate scenarios. Thus, we used the outputs of four models to provide the final phenophase projection. Among four models, the Alternating was found slightly better than other phenological models in capturing the variability in budburst and fruit-setting. This result was inconsistent with previous research results, which argued that the simpler the model structure (e.g. Uniforce model), the better the prediction performance of phenological models (Basler, 2016; Hufkens et al., 2018). But Darbyshire et al. (2016b) reported the Alternating model outperformed in explaining the variability in the full blossom stage of *'Cripps Pink'* apple than sequential model (Unchill model in our study), and was very suitable for application in future climates. Additionally, the performance of the M1 models coupled with photoperiod and temperature were not obviously improved compared with Uniforc

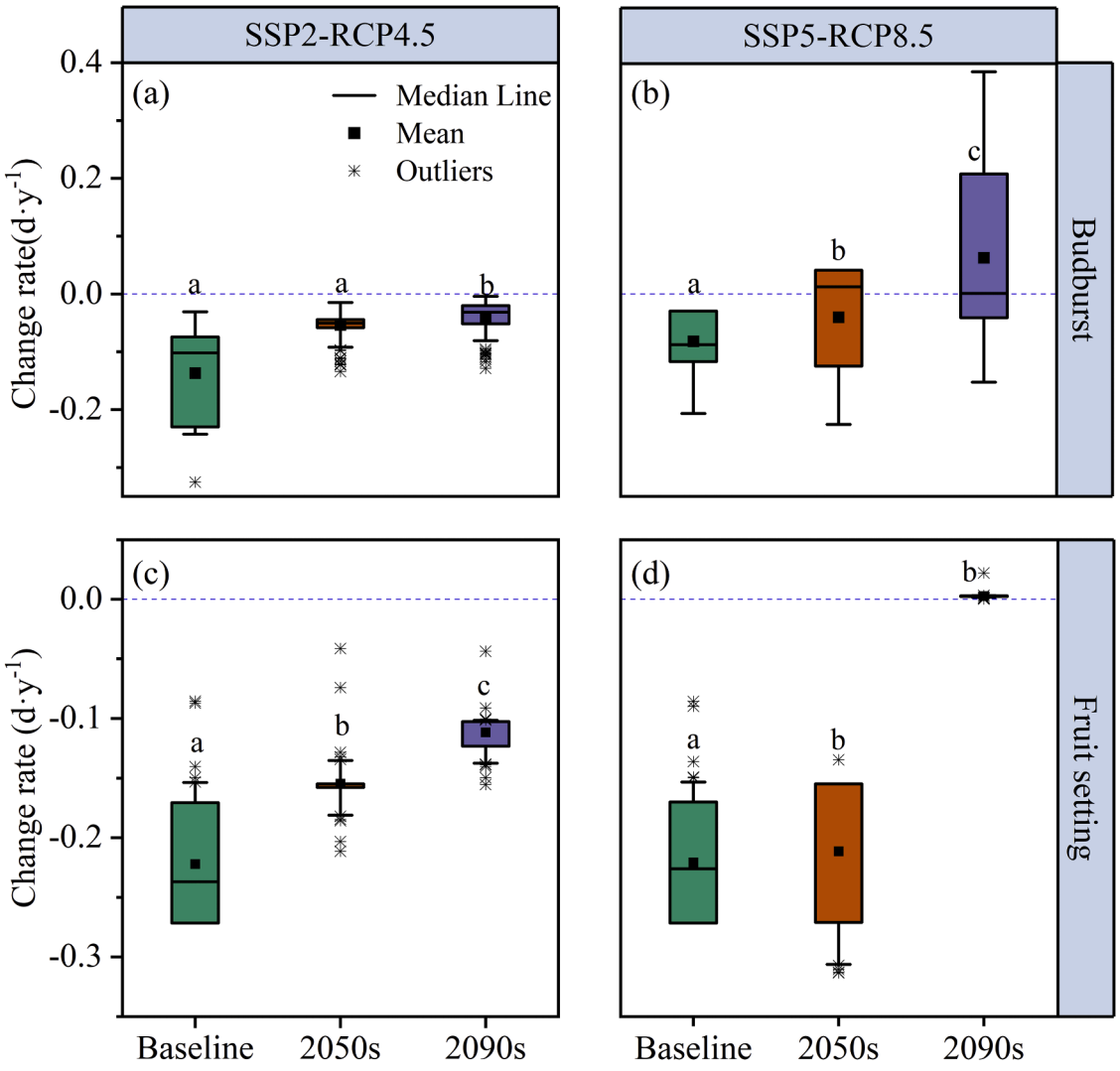

Fig. 5. Boxplots of the change rates of apple budburst (a-b) and fruit-setting dates (c-d) under SSP2-RCP4.5 and SSP5-RCP8.5 scenarios in the baseline (1981−2020), 2050s (2021−2060), and 2090s (2061−2100) periods in the Loess Plateau. Box boundaries indicated the 25th and 75th percentiles; the black line within the box marked the mean; black square marked the median; whiskers below and above the box were the 10th and 90th percentiles, respectively. Different lowercase letters indicate significant differences between different periods according to one-way ANOV tests followed by Tukey test at $p < 0.05$.

model based on temperature only. This may be because temperature plays a determining role in the appearance of apple phenological stages, while other factors are presumed to capture some of the remaining, unexplained variances (Heide and Prestrud, 2005; Legave et al., 2008). Similar to Alternating model, the Unichill model also takes chilling temperature into account during the endormancy phase on apple development, but the prediction performance of the model has not improved. This is attributed to the fact that Unichill model has up to eight parameters to optimize.

4.2. *Shifts of apple budburst and fruit-setting dates*

Model-based analysis showed apple budburst date occurred after March 15th (75 DOY), and fruit-setting date occurred after May 1st (120 DOY) in baseline period. This was in a comparable range of apple phenophases reported by Liu et al., (2020) and Wang et al., (2021) during the present period despite differences in region and varieties. The two phenophase was expected to advance by varying degrees under climate scenarios, and combinations of high-emission scenarios and 'far' time periods (SSP5-RCP8.5, 2090s) tended to advance larger than conservative scenarios and 'near' time periods (SSP2-RCP4.5, 2050s). For instance, budburst mean advance about 4.00 d and 4.39 d in 2050s under SSP2-RCP4.5 and SSP5-RCP8.5, while about 4.29 d and 8.24 d in 2090s under SSP2-RCP4.5 and SSP5-RCP8.5. However, budburst and fruit-setting would not always advance. In the southern edge of the Loess Plateau, an average delay of about 3.6 d was discovered in 2090s under SSP5-RCP8.5. It is likely that the raised temperature in winter higher than that in spring in the future periods, and it would take longer than normal for the chilling accumulation to complete, resulting in a corresponding delay occurrence in apple budburst. Additionally, differences also were seen in advancement rates of two phenophase between the two periods under climate scenarios. Overall annual advance rates of budburst decreased from 0.14 d in baseline period to 0.04 d in 2090s under SSP2-RCP4.5. From this can be concluded that the advancement in apple budburst was expected to become slower as the end of the century approached. Warmer winters resulted in reduced chilling, herein eventually slowed down the advancement of phenophase (Fraga and Santos, 2021; Hoffmann and Rath, 2013). Notably, the areas in which phenophase occurred later in baseline will advance larger. This indicated that areas with late phenology at current climate were more sensitive to future climate warming than areas with early phenology. Similar results were rarely reported in the literature. An explanation for this finding was the uneven changes of climate in the study area. The regions with late phenology stage usually had warmer winters and

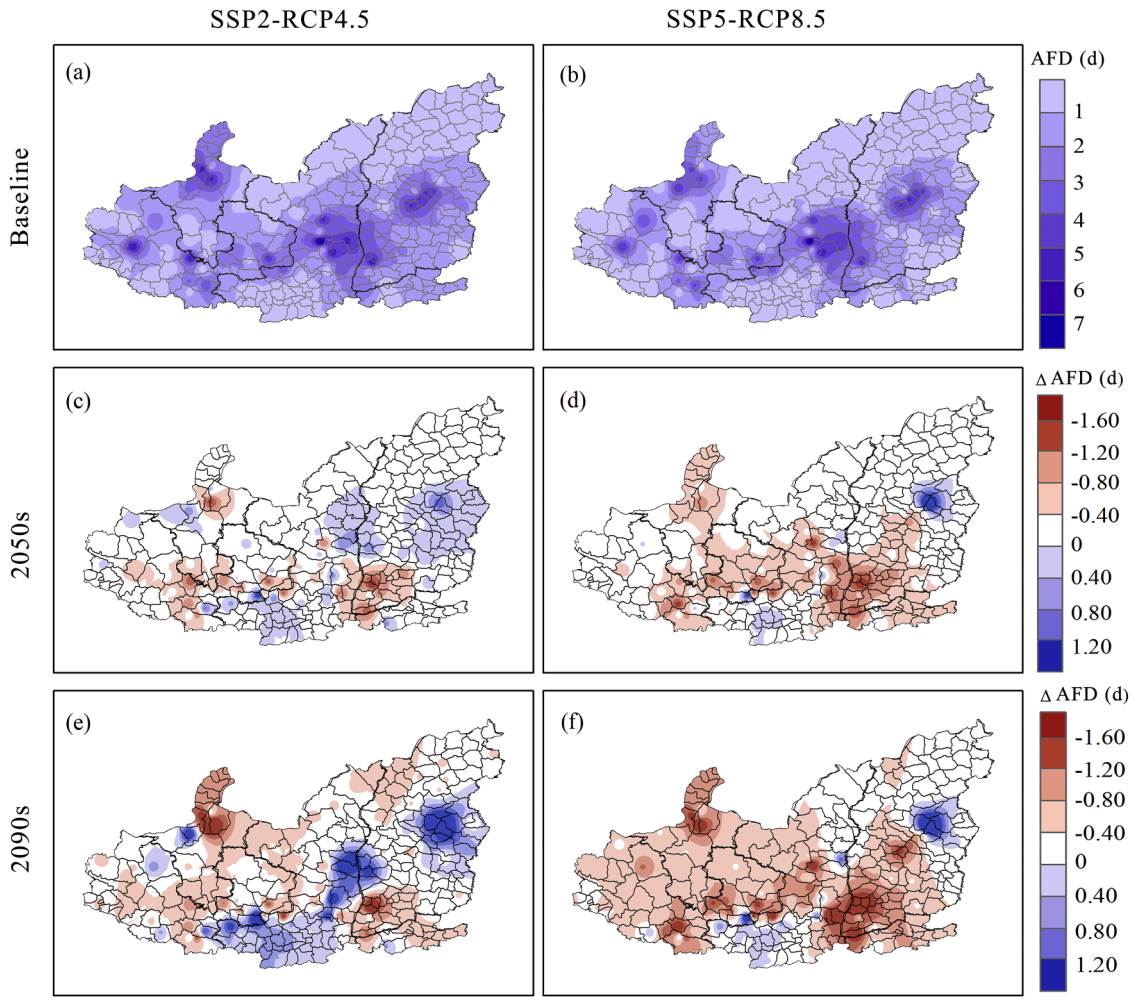

Fig. 6. Spatial distributions of frost frequency (accumulated frost days, AFD) in the period from apple budburst to fruit-setting date in the baseline of 1981-2020 under the emission scenarios of SSP2-RCP4.5 and SSP5-RCP8.5 (a-b), as well as the changes of AFD in future periods of 2050s (2021–2060; c-d) and 2090s (2061–2100; e-f) under the two scenarios. The AFD values were the average values of 40 years (Δ AFD= future-baseline).

cooler springs in the baseline period. However, warmer winter would become cooler, while cooler spring would become warmer in the future. Thus, apple chilling accumulation and heat forcing would complete earlier than the baseline, resulting in a large advancement of apple phenology. Compare with budburst, our results displayed relatively weaker advancing rates of fruit-setting. One proposed explanation for this result was that the temperature sensitivities of budburst stage to warming and chilling were greater than the fruit-setting stages (Li et al., 2016), while another was the short series of observation dataset of 2016−2020 caused an underestimation of influence of climate change on the fruit-setting stage, although the accuracy of the model was acceptable.

4.3. Shifts of late-spring frost frequency and intensity

Previous analyses of the effects of climate change on late-spring frost for temperate fruit trees usually neglected the problem of phenological window, whose length could heavily determine the sensitivity of fruit trees to frost injury. In this study, AFD and AFDD were calculated in the varying-length time intervals between apple budburst and fruit-setting dates in different future periods. In baseline period, AFD was at a low level in more than half of the Loess Plateau, however, AFDD was found severe in some central areas (Fig 6a, b; Fig 7a, b). Compared with the baseline, average AFD decreased in 2050s and 2090s under the two emission scenarios. Average AFDD increased under SSP2-RCP4.5, but increased first and then decreased under SSP5-RCP8.5. This result showed that rising temperature generally reduced the absolute number of frost events, while the severity of frost events was on an upward trajectory except in 2090s under SSP5-RCP8.5. Additionally, the areas with larger advancing of phenology stages were actually more susceptible to frost risks, more attention thus should be paid to these areas. This was due to the large advance in phenology is more likely to promote frost events overlapping the sensitive window from budburst to fruit-setting stage, and finally resulting in more frost risk (Hoffmann and Rath, 2013; Liu and Sherif, 2019; Parker et al., 2020). This finding indirectly corroborated that earlier phenophase in warmer climatic than current can lead to higher frequency or stronger frost damages (Augspurger, 2013; Mosedale et al., 2015; Sanguesa-Barreda et al., 2019). From the spatial perspective, the advancement in phenophase was disproportionately related to late-spring frost risks in the geographic distributions. Overall, spring late-frost risks remained unchanged or decreased in most northern and southern areas of the Loess Plateau under future climate change, but increased in some central areas. This was mainly because the reduction of chilling was stronger under the warming of the cooler climate in northern areas than under the warming of the warmer climate in central areas. Thus, the chilling accumulation would become less in northern areas than in central areas under future climate warming. Correspondingly, the forwarding of budburst/fruit-setting dates in northern areas was smaller than that in the central areas. This would further increase the encounter probability

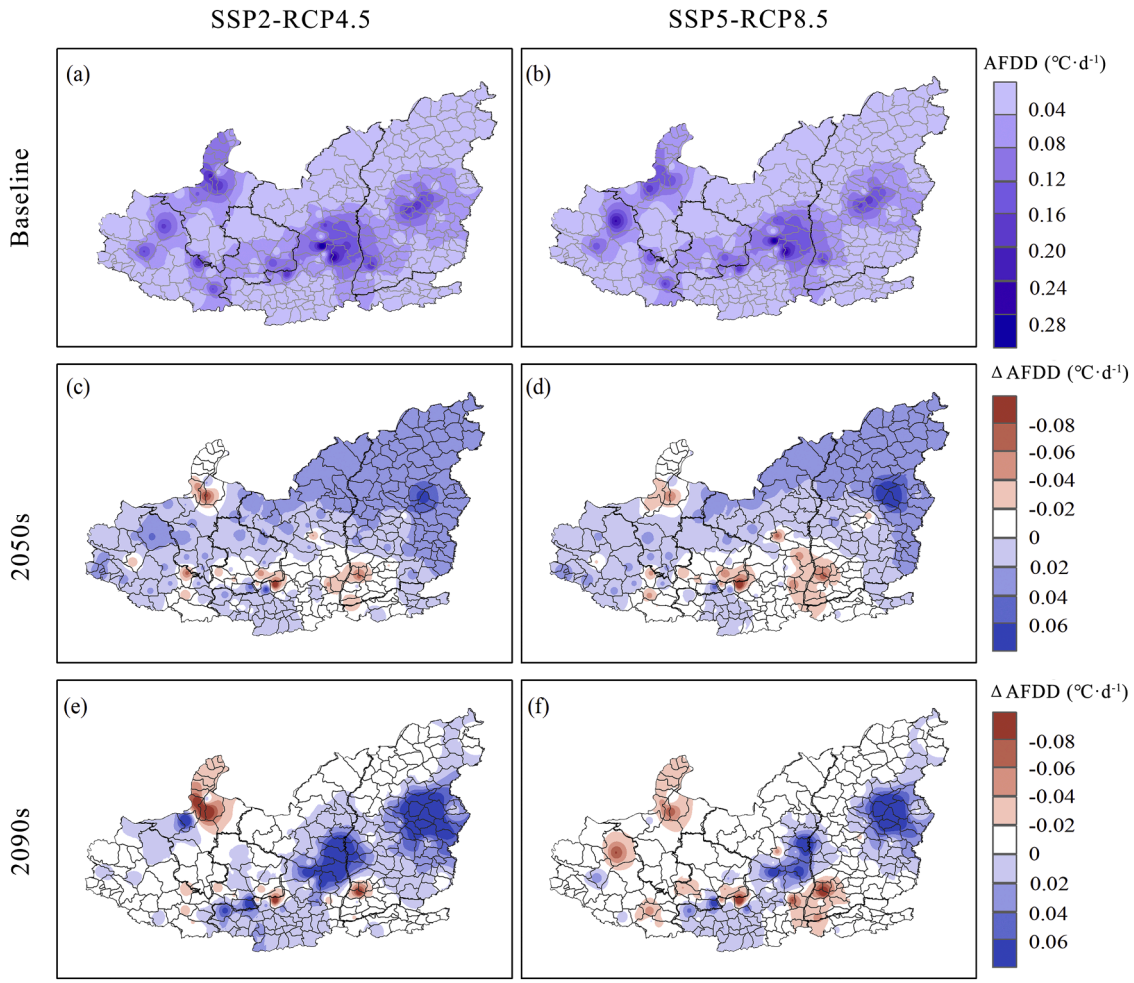

Fig. 7. Spatial distributions of frost intensity (accumulated frost degree-days, AFDD) in the period from apple budburst to fruit-setting date in the baseline of 1981-2020 under the SSP2-RCP4.5 and SSP5-RCP8.5 emission scenario (a-b), as well as the changes of AFDD in the periods of 2050s (2021–2060; c-d) and 2090s (2061–2100; e-f) under the two emission scenarios. The AFDD values were the average values of 40 years (Δ AFDD= future-baseline).

of late-spring frost and apple phenophase in the central areas. In comparison, the effect of reduced chilling was stronger in the central areas than in the southern areas. However, the effect of increased forcing overrode the effect of decreased chilling on the projected of budburst/fruit-setting in the cooler central areas than in the warmer southern areas under future climate warming. Ultimately, apple phenophases advanced smaller in the southern areas than in central areas. Similar findings were also found in a survey simulation of pecan in subtropical southeastern China (Zheng et al., 2021). They suggested that the risk of frost damage would increase in south areas since increased forcing offset the effect of decreased chilling on the projected timing of pecan phenophase, which partially supported the results of this study. For some central and southern areas (Xunyi, Yan'an, Zhuanglang county, and etc.) of the Loess Plateau, however, were still in the key areas for the development of apple production bases nowadays. Given that frost risk is expected to further increase in these regions, we advised that local policymakers and stakeholders should be more cautious when expanding local bases and scales of apple production. Nevertheless, due to the complex interactions between plant biological responses and climatic factors, it remains a challenge to more accurately determine the level of late-spring frost injury on apple production under future climate change. Thus, more continuous studies are needed to counteract the potential frost damage to apples. For example, it may be a good choice to use the phenological model dynamically coupled with frost hardiness model and calibrate the models based on more phenological observation data (Augspurger, 2013; Guillaume et al., 2018).

4.4. *Limitations and possible practice*

Our results showed that some major apple-producing areas in the Loess Plateau would suffer more severe frost intensity, especially in areas with larger advances in phenophase. However, some uncertainties and limitations remain. For example, there is a need for additional experimental to validate the changing trends in phenology and frost highlighted. New phenological observations are required for improving the reliability of the phenological simulation, especially for fruit-setting stage affected in this study by the limited data availability. Other weather factors that affect frost events, such as relative humidity, wind, etc., also need to be considered. Therefore, when interpreting our results, it should be noted that we only pointed out the potential risks of late-spring frost in the future, rather than providing completely reliable forecasts. Nonetheless, our findings may help promote preventive interventions in the most critical areas identified in the Loess Plateau of China to mitigate future yield/quality losses and ensure future sustainability. Recommendations for practices that mitigate frost include wind machines, heaters/smudge pots, sprinklers, and sprayable compounds to delay bloom. But these practices may not be sufficient for the severity of the different climate scenarios, e.g., under SS5-RCP8.5, orchard relocation may also be necessary for the most affected areas. Considering economic and labor costs, orchard planning in areas dominated by increased frost should avoid low-lying fields where cold air tends to flow into and remain trapped. Planting late-flowering varieties or delaying removal of straw mulch may be ideal.

5. Conclusions

Our study represents the first attempt to assess late-spring frost based on phenological dynamics in apple tree in the Loess Plateau, and thus a new step towards understanding the local frost risk dynamics of climate change. Apple budburst and fruit-setting were expected to advance by varying degrees, and combinations of high-emission scenarios and 'far' time periods (SSP5-RCP8.5, 2090s) advance larger than conservative scenarios and 'near' time periods (SSP2-RCP4.5, 2050s). Advancement rates of two phenophase were decreasing as the end of the century approached. Frost frequency was projected to decrease under future scenarios, while frost intensity was on an upward trajectory (Except for SSP5-RCP8.5, 2090s). Due to the different directions of changes in frost intensity and frequency, the projected increase frost risk is mainly across the central areas of the study areas, and the unchanged or decreased frost risk distribute in the northern and southern areas of the study areas. Additionally, the advancement in phenophase is disproportionately related to late-spring frost risks in the geographic distributions. The central areas of the Loess Plateau with relative late phenology in baseline were found to advance more under future scenarios, where would suffer from greater frost risk.

Credit Author Statement

Xiaoya Ru: Conceptualization, Methodology, Software, Coding, Calibration, Validation, Writing – original draft. Yuan Jiang: Calibration, Validation. Qi Luo: Calibration, Validation. Runhong Wang: Methodology, Visualization. Xinxin Feng: Methodology, Resources. Jinghong Wang: Software. Zhao Wang: Project supervision, Funding acquisition. Meirong Li: Methodology, Data Curation. Zhenjiang Qu: Methodology, Resources. Baofeng Su: review & editing. Hao Feng: Funding acquisition, review & editing. Dong Zhang: review & editing. Deli Liu: review & editing, Research administration. Qiang Yu: review & editing. Jianqiang He: Methodology, review & editing, Funding acquisition.

Declaration of Competing Interest

The authors declare that they have no known competing financial interests or personal relationships that could have appeared to influence the work reported in this paper.

Data availability

Data will be made available on request.

Acknowledgments

This research was partially supported by the National Natural Science Foundation of China (No. 52079115, 41961124006), the National Key R&D Program of China (No. 2021YFD190070402, 2017RFD0300300), the Key Research and Development Program of Shaanxi (No. 2019ZDLNY07-03), the Open Project Fund from the Key Laboratory of Eco-Environment and Meteorology for the Qinling Mountains and Loess Plateau, Shaanxi Provincial Meteorological Bureau (No. 2019Z-5), and the "111 Project" (No. B12007) of China. The author would like to thank Chinese Meteorological Administration (CMA) for providing the meteorological data. Thanks to Dr. Bernie Dominiak for his editing and review of the manuscript.

Supplementary materials

Supplementary material associated with this article can be found, in the online version, at doi:10.1016/j.scienta.2022.111604.

References

Augspurger, C.K., 2013. Reconstructing patterns of temperature, phenology, and frost damage over 124 years: spring damage risk is increasing. Ecology 94, 41–50. https://doi.org/10.1890/12-0200.1.

Basler, D., 2016. Evaluating phenological models for the prediction of leaf-out dates in six temperate tree species across central Europe. Agric. For. Meteorol. 217, 10–21. https://doi.org/10.1016/j.agrformet.2015.11.007.

Baumgarten, F., Zohner, C.M., Gessler, A., Vitasse, Y., 2021. Chilled to be forced: the best dose to wake up buds from winter dormancy. N. Phytol. 230, 1366–1377. https://doi.org/10.1111/nph.17270.

Blümel, K., Chmielewski, F.M., 2012. Shortcomings of classical phenological forcing models and a way to overcome them. Agric. For. Meteorol. 164, 10–19. https://doi.org/10.1016/j.agrformet.2012.05.001.

Byrd, R.H., Lu, P., Nocedal, J., Zhu, C., 1995. A limited memory algorithm for bound constrained optimization. SIAM J. Sci. Comput. 16, 1190–1208. https://doi.org/10.1137/0916069.

Cannell, M., 1986. Climatic warming, spring budburst and frost damage on trees. J. Appl. Ecol. 23 https://doi.org/10.2307/2403090.

Cannell, M., Smith, R., 1983. Thermal time, chill days and prediction of budburst in Picea sitchensis. J. Appl. Ecol. 951–963. https://doi.org/10.2307/2403139.

Chapman, P., Catlin, G., 1976. Growth stages in fruit trees-from dormant to fruit set. New York's Food and. Life Sciences Bulletin 58.

Chuine, I., 2000. A Unified Model for Budburst of Trees. J. Theor. Biol. 207, 337–347. https://doi.org/10.1006/jtbi.2000.2178.

Coupled Model Intercomparison Project Phase 6, 2021. https://esgf-node.llnl.gov/projects/cmip6/.

Darbyshire, R., Measham, P., Goodwin, I., 2016a. A crop and cultivar-specific approach to assess future winter chill risk for fruit and nut trees. Clim. Change 137, 541–556. https://doi.org/10.1007/s10584-016-1692-3.

Darbyshire, R., Pope, K., Goodwin, I., 2016b. An evaluation of the chill overlap model to predict flowering time in apple tree. Sci. Hortic. 198, 142–149. https://doi.org/10.1016/j.scienta.2015.11.032.

Deng, G., Zhang, H., Yang, L., Zhao, J., Guo, X., Ying, H., Rihan, W., Guo, D., 2020. Estimating frost during growing season and its impact on the velocity of vegetation greenup and withering in Northeast China. Remote Sens 12, 1355–1372. https://doi.org/10.3390/rs12091355.

Dennis, F.G., 2003. Problems in standardizing methods for evaluating the chilling requirements for the breaking of dormancy in buds of woody plants. Hortscience 38, 347–350. https://doi.org/10.21273/HORTSCI.38.3.347.

Eccel, E., Rea, R., Caffarra, A., Crisci, A., 2009. Risk of spring frost to apple production under future climate scenarios: the role of phenological acclimation. Int. J. Biometeorol. 53, 273–286. https://doi.org/10.1007/s00484-009-0213-8.

Eyring, V., Bony, S., Meehl, G.A., Senior, C.A., Stevens, B., Stouffer, R.J., Taylor, K.E., 2016. Overview of the coupled model intercomparison project phase 6 (CMIP6) experimental design and organization. Geosci. Model Dev. 9 https://doi.org/10.5194/gmd-9-1937-2016, 1937-1958.

Farajzadeh, M., Rahimi, M., Kamali, G.A., Mavrommatis, T., 2010. Modelling apple tree bud burst time and frost risk in Iran. Meteorol. Appl. 17, 45–52. https://doi.org/10.1002/met.159.

Fraga, H., Santos, J.A., 2021. Assessment of climate change impacts on chilling and forcing for the main fresh fruit regions in Portugal. Front. Plant Sci 12, 689121. https://doi.org/10.3389/fpls.2021.689121.

Guak, S., Neilsen, D., 2013. Chill unit models for predicting dormancy completion of floral buds in apple and sweet cherry. Hort. Environ. Biotechnol. 54, 29–36. https://doi.org/10.1007/s13580-013-0140-9.

Gubernatis, J.E., 2005. Marshall Rosenbluth and the Metropolis algorithm. Phys. Plasma 12, 057303. https://doi.org/10.1063/1.1887186.

Guillaume, C., Isabelle, C., Marc, B., Thierry, A., 2018. Assessing frost damages using dynamic models in walnut trees: exposure rather than vulnerability controls frost risks. Plant Cell Environ. 41, 1008–1021. https://doi.org/10.1111/pce.12935.

Guo, L., Wang, J., Li, M., Liu, L., Xu, J., Cheng, J., Gang, C., Yu, Q., Chen, J., Peng, C., Luedeling, E., 2019. Distribution margins as natural laboratories to infer species' flowering responses to climate warming and implications for frost risk. Agric. For. Meteorol. 268, 299–307. https://doi.org/10.1016/j.agrformet.2019.01.038.

Hastings, W.K., 1970. Monte Carlo sampling methods using Markov chains and their applications. Biometrika 57, 97–109. https://doi.org/10.1093/biomet/57.1.97.

Hawerroth, F.J., Herter, F.G., Petri, J.L., Marafon, A.C., Leonetti, J.F., 2013. Evaluation of winter temperatures on apple budbreak using grafted twigs. Rev Bras Frutic 35, 713–721. https://doi.org/10.1590/S0100-29452013000300007.

Heide, O., Prestrud, A., 2005. Low temperature, but not photoperiod, controls growth cessation and dormancy induction and release in apple and pear. Tree Physiol 25, 109–114. https://doi.org/10.1093/treephys/25.1.109.

Hoffmann, H., Rath, T., 2013. Future bloom and blossom frost risk for Malus domestica considering climate model and impact model uncertainties. PLoS ONE 8, 75033–75046. https://doi.org/10.1371/journal.pone.0075033.

Houston, L., Capalbo, S., Seavert, C., Dalton, M., Bryla, D., Sagili, R., 2017. Specialty fruit production in the Pacific Northwest: adaptation strategies for a changing climate. Clim. Change 146, 159–171. https://doi.org/10.1007/s10584-017-1951-y.

Hufkens, K., Basler, D., Milliman, T., Melaas, E.K., Richardson, A.D., Goslee, S., 2018. An integrated phenology modelling framework in R. Methods Ecol. Evol. 9, 1276–1285. https://doi.org/10.1111/2041-210x.12970.

IPCC, 2021: Climate change 2021: the physical science basis. Contribution of working group I to the sixth assessment report of the intergovernmental panel on climate change [Masson-Delmotte, V., P. Zhai, A. Pirani, S.L. Connors, C. Péan, S. Berger, N. Caud, Y. Chen, L. Goldfarb, M.I. Gomis, M. Huang, K. Leitzell, E. Lonnoy, J.B.R.

Matthews, T.K. Maycock, T. Waterfield, O. Yelekçi, R. Yu, and B. Zhou (eds.)]. Cambridge University Press, Cambridge, United Kingdom and New York, NY, USA, In press, doi:10.1017/9781009157896.
Kaufmann, H., Blanke, M.M., 2019. Chilling requirements of Mediterranean fruit crops in a changing climate. Acta Hortic. 275–280. https://doi.org/10.17660/ActaHortic.2019.1242.38.
Kaukoranta, T., Tahvonen, R., Ylämäki, A., 2010. Climatic potential and risks for apple growing by 2040. Agric. Food Sci. 19, 144–159. https://doi.org/10.2137/145960610791542352.
Kramer, K., 1994. Selecting a model to predict the onset of growth of Fagus sylvatica. J. Appl. Ecol. 31, 172–181. https://doi.org/10.2307/2404609.
Labe, Z., Ault, T., Zurita-Milla, R., 2016. Identifying anomalously early spring onsets in the CESM large ensemble project. Clim. Dyn. 48, 3949–3966. https://doi.org/10.1007/s00382-016-3313-2.
Lamichhane, J.R., 2021. Rising risks of late-spring frosts in a changing climate. Nat. Clim. Change 11, 554–555. https://doi.org/10.1038/s41558-021-01090-x.
Legave, J.M., Farrera, I., Almeras, T., Calleja, M., 2008. Selecting models of apple flowering time and understanding how global warming has had an impact on this trait. J. Hortic. Sci. Biotechnol. 83, 76–84. https://doi.org/10.1080/14620316.2008.11512350.
Li, X., Jiang, L., Meng, F., Wang, S., Niu, H., Iler, A.M., Duan, J., Zhang, Z., Luo, C., Cui, S., Zhang, L., Li, Y., Wang, Q., Zhou, Y., Bao, X., Dorji, T., Li, Y., Penuelas, J., Du, M., Zhao, X., Zhao, L., Wang, G., 2016. Responses of sequential and hierarchical phenological events to warming and cooling in alpine meadows. Nat. Commun. 7, 12489. https://doi.org/10.1038/ncomms12489.
Liu, D.L., Zuo, H., 2012. Statistical downscaling of daily climate variables for climate change impact assessment over New South Wales. Australia. Clim. Change 115, 629–666. https://doi.org/10.1007/s10584-012-0464-y.
Liu, J., Sherif, S.M., 2019. Combating spring frost with ethylene. Front. Plant Sci. 10 https://doi.org/10.3389/fpls.2019.01408, 1408-1408.
Liu, L., Wang, J., Bai, Q., 2020. Impact of climate changes on apple's phenophases in the main producing areas of the Loess Plateau in China. Int. J. Fruit Sci. 37, 330–338, 10.139250.cnki.gsxb.20190254.
Masaki, Y., 2019. Future risk of frost on apple trees in Japan. Clim. Change 159, 407–422. https://doi.org/10.1007/s10584-019-02610-7.
Mbovora, S.M., Musvosvi, C., Gasura, E., Okatan, V., 2021. Morphological diversity among accessions of apple tree (Malus × Domestica Borkh). Adv. Agron. 2021, 1–16. https://doi.org/10.1155/2021/7705856.
Migliavacca, M., Sonnentag, O., Keenan, T.F., Cescatti, A., O'Keefe, J., Richardson, A.D., 2012. On the uncertainty of phenological responses to climate change, and implications for a terrestrial biosphere model. Biogeosciences 9, 2063–2083. https://doi.org/10.5194/bg-9-2063-2012.
Mosedale, J.R., Wilson, R.J., Maclean, I.M., 2015. Climate change and crop exposure to adverse weather: changes to frost risk and grapevine flowering conditions. PLoS ONE 10, e0141218. https://doi.org/10.1371/journal.pone.0141218.
Parker, L., Pathak, T., Ostoja, S., 2020. Climate change reduces frost exposure for high-value California orchard crops. Sci. Total Environ. 762, 143971 https://doi.org/10.1016/j.scitotenv.2020.143971.
Pfleiderer, P., Menke, I., Schleussner, C.F., 2019. Increasing risks of apple tree frost damage under climate change. Clim. Change 157, 515–525. https://doi.org/10.1007/s10584-019-02570-y.
Powell, L.E., 1986. The chilling requirement in apple and its role in regulating time of flowering in spring in cold-winter climates. Acta Hortic 179, 129–140. https://doi.org/10.17660/ActaHortic.1986.179.10.
Qiu, M., Liu, B., Liu, Y., Wang, K., Pang, J., Zhang, X., He, J., 2020. Simulation of first flowering date for apple and risk assessment of late frost in main producing areas of northern China (in Chinese with English abstract). Transactions of the CSAE 36, 154–163. https://doi.org/10.11975/j.issn.1002-6819.2020.21.01.
Qu, Z., Zhou, G., 2016. Climate suitability for potential Fuji apple cultivation in China (in Chinese with English abstract). Acta Meteorol. Sin. 74, 479–490. https://doi.org/10.11676/qxxb2016.027.
Sanguesa-Barreda, G., Villalba, R., Rozas, V., Christie, D.A., Olano, J.M., 2019. Detecting nothofagus pumilio growth reductions induced by past spring frosts at the Northern Patagonian Andes. Front Plant Sci 10, 1413. https://doi.org/10.3389/fpls.2019.01413.
Shaanxi Fruits Industry, 2014. http://www.guoye.sn.cn/.
Shaanxi Meteorological Bureau, 2017. http://sn.cma.gov.cn/.
Smith, M., 1986. Climatic warming, spring budburst and forest damage on trees. J. Appl. Ecol. 23, 177–191. https://doi.org/10.2307/2403090.
Taylor, S.D., 2018. PyPhenology: a python framework for plant phenology modelling. J. Open Source Softw. 3 https://doi.org/10.21105/joss.00827, 827.
The National Meteorological Information Center, 2014. http://data.cma.cn/.
Unterberger, C., Brunner, L., Nabernegg, S., Steininger, K.W., Steiner, A.K., Stabentheiner, E., Monschein, S., Truhetz, H., 2018. Spring frost risk for regional apple production under a warmer climate. PLoS ONE 13. https://doi.org/10.1371/journal.pone.0200201.
Wales, D.J., Doye, J.P., 1997. Global optimization by basin-hopping and the lowest energy structures of Lennard-Jones clusters containing up to 110 atoms. J. Phys. Chem. A. 101, 5111–5116. https://doi.org/10.1021/jp970984n.
Wang, M., Liu, B., Liu, Y., Yang, X., Han, S., Qiu, M., Li, Q., 2020a. Assessment on the freezing Injury risk during apple flowering in Liquan and Xunyi (in Chinese with English abstract). Chinese J. Agrometeorol. 41, 381–392. https://doi.org/10.3969/j.issn.1000-6362.2020.06.005.
Wang, S., An, J., Zhao, X., Gao, X., Wu, P., Huo, G., Robinson, B.H., 2020b. Age- and climate- related water use patterns of apple trees on China's Loess Plateau. J. Hydrol. 582, 124462 https://doi.org/10.1016/j.jhydrol.2019.124462.
Wang, R., Ru, X., Jiang, T., Wang, J., Wang, Z., Su, B., Zhang, D., Yu, Q., Feng, H., He, J., 2021. Based on the phenological model to study the possible changes of apple flowering dates under future climate scenarios in Shaanxi Province. Chin. J. Agrometeorol. 42, 729–745.
Weinberger, J.H., 1950. Chilling requirements of peach varieties. Proc. Am. Soc. Hortic. Sci. 56, 122–128.
Xavier, M., Isabelle, C., 2014. Will tree species experience increased frost damage due to climate change because of changes in leaf phenology? Can. J. For. Res. 44, 1555–1565. https://doi.org/10.1139/cjfr-2014-0282.
Xiao, L., Liu, L., Asseng, S., Xia, Y., Tang, L., Liu, B., Cao, W., Zhu, Y., 2018. Estimating spring frost and its impact on yield across winter wheat in China. Agric. For. Meteorol. 154–164. https://doi.org/10.1016/j.agrformet.2018.06.006, 260-261.
Yaacoubi, A.E., Oukabli, A., Hafidi, M., Farrera, I., Ainane, T., Cherkaoui, S.I., Legave, J.-.M., 2019. Validated model for apple flowering prediction in the Mediterranean area in response to temperature variation. Sci. Hortic. 249, 59–64. https://doi.org/10.1016/j.scienta.2019.01.036.
Yan, B., Pascual, J., Bouchard, M., D'Orangeville, L., Perie, C., Girardin, M.P., 2021. Multi-model projections of tree species performance in Quebec, Canada under future climate change. Global Change Biol. https://doi.org/10.1111/gcb.16014.
Zhang, R., Lin, J., Wang, F., Shen, S., Wang, X., Rao, Y., Wu, J., Hänninen, H., 2021. The chilling requirement of subtropical trees is fulfilled by high temperatures: a generalized hypothesis for tree endodormancy release and a method for testing it. Agric. For. Meteorol. 298–299. https://doi.org/10.1016/j.agrformet.2020.108296, 108296.
Zhang, X., 2007. A comparison of explicit and implicit spatial downscaling of GCM output for soil erosion and crop production assessments. Clim. Change 84, 337–363. https://doi.org/10.1007/s10584-007-9256-1.
Zheng, B., Chapman, S.C., Christopher, J.T., Frederiks, T.M., Chenu, K., 2015. Frost trends and their estimated impact on yield in the Australian wheatbelt. J. Exp. Bot. 66, 3611–3623. https://doi.org/10.1093/jxb/erv163.
Zheng, J., Hanninen, H., Lin, J., Shen, S., Zhang, R., 2021. Extending the cultivation area of pecan (Carya illinoinensis) toward the south in southeastern subtropical China may cause increased cold damage. Front. Plant Sci. 12, 768963 https://doi.org/10.3389/fpls.2021.768963.